

# Magnetic state control of ferromagnetic nanodots by magnetic force microscopy probe

Joonyeon Chang<sup>a)</sup>

*Future Technology Research Divisions, Korea Institute of Science and Technology, Seoul 136-791, Korea*

V. L. Mironov, B. A. Gribkov, A. A. Fraerman, S. A. Gusev, and S. N. Vdovichev

*Institute for Physics of Microstructures, RAS, GSP-105, 603950 Nizhny Novgorod, Russia*

(Received 20 February 2006; accepted 2 September 2006; published online 16 November 2006)

We present the magnetic state control of individual ferromagnetic nanodots under inhomogeneous magnetic field induced by the probe of magnetic force microscope (MFM). Arrays of submicron sized elliptical ferromagnetic Co and FeCr dots with different sizes and periods were fabricated to demonstrate addressable manipulation of magnetization. MFM observations show the magnetization reversal and processes of local remagnetization of individual ferromagnetic nanodots subjected to magnetic change. Computer simulation of magnetization processes under inhomogeneous magnetic field induced by MFM probe was performed on the base of Landau-Lifshitz-Gilbert equation for magnetization. © 2006 American Institute of Physics. [DOI: 10.1063/1.2384811]

## I. INTRODUCTION

Characterization and understanding of magnetic properties of ferromagnetic nanodots with well defined periodicity have been a major challenge for decades in the areas of magnetic recording media with ultrahigh density and magnetic devices.<sup>1</sup> Recently, much attention has been focused on the study of magnetization process of individual magnetic nanodot directly under the magnetic field of the magnetic force microscopy (MFM) probe. For example, only uniform states (USs) with opposite directions of magnetization are possible in a small single domain anisotropic dot. Vortex state (VS) is realized in a dot with geometrical size above critical length.<sup>2-5</sup> Uniform states are also possible in such ferromagnetic nanodots as metastable states.<sup>6</sup> Different distribution of magnetic state of a few nanodots in array structure is a good source of an inhomogeneous magnetic field.

Amplitude of this inhomogeneous magnetic field is about the saturation magnetic moment  $M_s$  of the ferromagnet and a scale of the field variation is determined by period of particle array. For typical transition metals value  $M_s$  is about 1000 G and the modern lithographic techniques allow one to vary the particle lattice period over a wide range from 10 to 1000 nm. In addition, the magnetic field distribution can be varied by magnetizing or demagnetizing whole dot array or some of its parts.

Controllable inhomogeneous magnetic field induced by the dots leads to substantial change in transport properties of superconductors<sup>7-10</sup> and Josephson junctions.<sup>11-13</sup> Recently, it was shown that inhomogeneous magnetic field produced by a ferromagnetic island acts as an effective potential that can efficiently trap spin polarized carriers in the system with giant Zeeman splitting.<sup>14</sup> Giant  $g$  factor was observed, for example, in diluted magnetic semiconductors.<sup>15</sup> Investigation of influence of spin injection from ferromagnetic dots on

transport properties of superconductors<sup>16-19</sup> and semiconductors<sup>20</sup> is another interesting field for application of ferromagnetic dots.

One possibility to manipulate the magnetic state of ferromagnetic nanodots is magnetization reversal under the probe of magnetic force microscope. In this case, magnetic state of each selected element can be controlled by approaching the MFM probe to a specific dot independently. In such a way, we can create different distributions of magnetization in an array of ferromagnetic dots, which can be useful for various applications. Moreover, magnetic tip induces inhomogeneous magnetic field and magnetization reversal has additional peculiarities in comparison with the process in uniform external magnetic field. Regardless of the fact that influence of magnetic tip on state of ferromagnetic dots was experimentally investigated earlier,<sup>21-24</sup> the problem still needs further study. In this work, we investigated both theoretically and experimentally remagnetization processes in ferromagnetic Fe-Cr and Co nanodots under inhomogeneous magnetic field induced by magnetic tip of MFM, which allow to produce inhomogeneous magnetic field sources based on nanodot arrays.

## II. EXPERIMENTAL PROCEDURES

The rectangular lattices of elliptical Co dots with different sizes and different periods were fabricated by the electron-beam lithography and subsequent ion etching of thin Co films.<sup>25</sup> The unique one to be noticed is to use fullerene consisting of  $C_{60}$  molecules as an electron-beam resist which acts as a patterning medium as well as a robust mask for ion etching. The characteristic lateral sizes of dots are varied in the range of 150–600 nm (aspect ratio in the range of 1.5–2.5), and heights of dots were 10–30 nm. Array of FeCr dots was fabricated by four beam interference laser annealing of thin composite FeCr films.<sup>26</sup> Since both dots were coated with a thin Ti layer deposited in the same vacuum chamber

<sup>a)</sup>Author to whom correspondence should be addressed; FAX: 82-2-958-5431; electronic mail: presto@kist.re.kr

without breaking vacuum condition, the surface was well protected from oxygen. The dots showed good stability of magnetic properties over a few months.

The distribution of remanent magnetization and processes of local remagnetization were studied using a multi-mode Scanning Probe Microscopy (SPM) Solver-PRO (NT-MDT). MFM measurements were performed in the noncontact constant height mode and the standard double pass tapping/lift mode. Standard Co-coated silicon cantilevers (MicroMash) magnetized along the tip axis prior to magnetic imaging were used in the MFM experiments. The phase shift of cantilever oscillations under the gradient of magnetic field was registered as the MFM contrast.

### III. COMPUTER SIMULATIONS

Modeling of remagnetization processes in ferromagnetic nanodots under MFM probe magnetic field was performed on the base of Landau-Lifshitz-Gilbert (LLG) equation for magnetization  $\mathbf{M}(\mathbf{r}, t)$ :

$$\frac{\partial \mathbf{M}}{\partial t} = -\frac{\gamma}{1 + \alpha^2} [\mathbf{M} \mathbf{H}_{\text{eff}}] - \frac{\alpha \gamma}{(1 + \alpha^2) M_s} [\mathbf{M} [\mathbf{M} \mathbf{H}_{\text{eff}}]], \quad (1)$$

where  $\gamma$  is the gyromagnetic ratio,  $\alpha$  is the dimensionless damping parameter, and  $M_s$  is the magnetic moment in saturation. The effective field  $\mathbf{H}_{\text{eff}} = -\delta E / \delta \mathbf{M}$  is a variation derivative of the energy function. The total energy of the particle can be defined by

$$E = E_{\text{ex}} + E_m + E_h. \quad (2)$$

The first term  $E_{\text{ex}}$  is the energy of the exchange interaction, the second term  $E_m$  is the demagnetization energy of the dots. Expressions for these terms have conventional form.<sup>27</sup> The last term  $E_h$  is the energy of the interaction between the magnetic moment and the nonuniform external magnetic field  $\mathbf{H}$ . In calculations the MFM probe was approximated as a single dipole<sup>28,29</sup> with effective magnetic moment  $m_{\text{eff}} = M_{\text{sp}} V_{\text{eff}}$  ( $M_{\text{sp}}$  is the remanent magnetization of capping material,  $V_{\text{eff}}$ —the effective volume of the interactive part of magnetic layer). We studied redistribution of magnetization during probe moving across the dots. At each stage stationary solutions of the LLG equations for the particles in the inhomogeneous field of MFM probe have been found for selected probe positions. Afterwards the probe has been replaced in the next position and LLG equations have been solved again with previous magnetization distribution used as the initial state for the next step computation.

To avoid a three-dimensional grid problem, which needs large computer resources, we assumed that magnetization of a cylindrical dot does not depend on the coordinate  $z$  along the cylindrical axis. Then we integrated the relations for the energy over  $z$  and obtained the energy as a function of the magnetization, which is a function of only two space variables. The effective field  $\mathbf{H}_{\text{eff}}$  does not depend on  $z$  either, so we have a three-dimensional problem reduced to the two-dimensional one. To develop a numerical method we divided the dot into rectangular parallelepipeds with a square base of size  $\delta$  in the plane  $x, y$  and of height  $h$  and obtained approximate expressions for different parts of the energy function

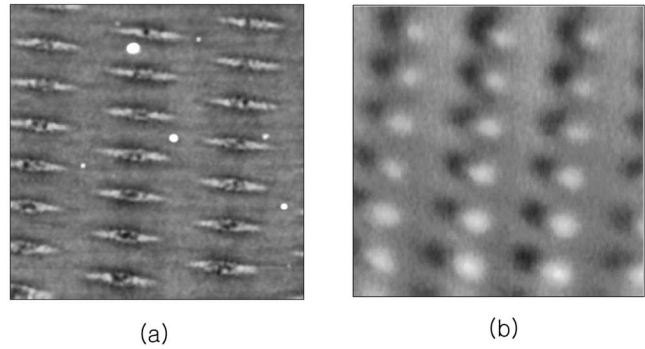


FIG. 1. AFM (a) and constant height MFM (b) images of FeCr dot array. Scan area is  $4 \times 4 \mu\text{m}^2$ .

using the grid values of magnetization  $\mathbf{M} = \{M_x, M_y, M_z\}$ . We chose the cell size considering two factors. (1), The size of the cell should be smaller than the characteristic exchange length  $\sqrt{J/M_s^2}$  ( $J$  is constant of exchange interaction) in order to describe the inhomogeneous magnetization correctly. (2) We cannot make it very small because of the computation time limitations. So in calculations value of cell  $\delta$  was less than 20 nm. All calculations were carried out for parameters of cobalt  $J = 10^{-6}$  erg/cm,  $M_s = 1400$  G, and  $V_{\text{eff}} = 1.25 \times 10^{-16}$  cm<sup>3</sup>. We omitted magnetocrystalline anisotropy term in (2), assuming polycrystalline structure of the dot.

### IV. RESULTS AND DISCUSSION

#### A. MFM probe induced $\text{US}_R \leftrightarrow \text{US}_L$ transitions

The MFM induced magnetization reversal in elliptical Co dots was observed by Kleiber *et al.*<sup>21</sup> The dots were placed in the external demagnetizing field less than critical field and actually the MFM probe was used to initiate switching of magnetization between uniform states with right ( $\text{US}_R$ ) and left ( $\text{US}_L$ ) orientations. Afterwards, authors<sup>22,23</sup> performed more detailed investigations showing that reorientation effects depend on the probe position relative to dot. They showed that the probe manipulation across the dot can lead to the magnetization reversal and, in particular, possibility of one touch remagnetization by MFM probe with high magnetic moment was demonstrated. In this part, we consider in detail magnetization reversal processes under inhomogeneous magnetic field of MFM probe moving along the ferromagnetic dot.

We investigated MFM induced magnetization reversal processes in the high aspect ratio FeCr dots of which size is  $280 \times 700$  nm<sup>2</sup>. Atomic force microscopy (AFM) and MFM (constant height mode) images of the sample are presented in Fig. 1. The dots have lentil-like shape clearly seen in Fig. 1(a). Separation between dots is about 500 nm. The sample was previously magnetized in the long axis direction. The magnetic state of dots [Fig. 1(b)] corresponds to the uniform distribution of magnetization. As shown in experiments, VS practically was not realized in such high aspect ratio dots.

The micromagnetic simulations show that the reversal  $\text{US}_R \leftrightarrow \text{US}_L$  process is accompanied by very complicated redistribution of dot magnetization. The step-by-step stages of remagnetization under MFM probe moving across the edge

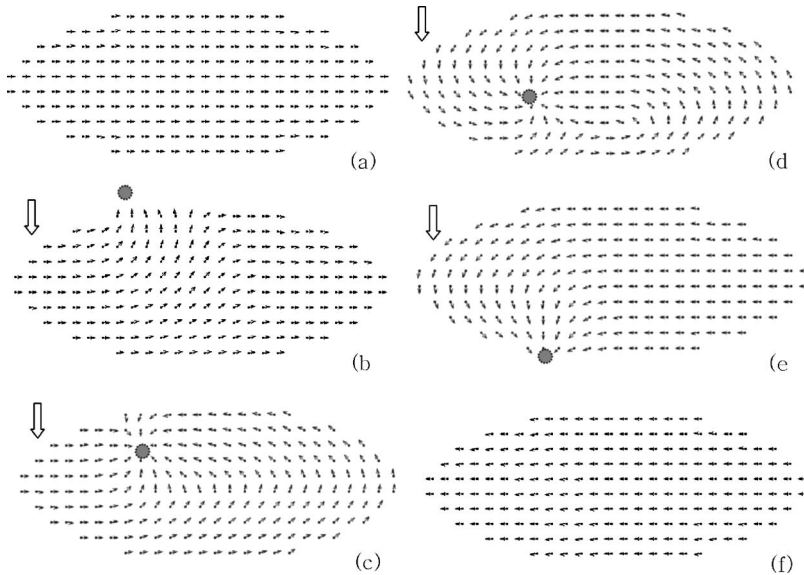


FIG. 2. Step-by-step stages of reversal  $US_R \leftrightarrow US_L$  process under MFM probe moving across the dot (the probe position indicated by a gray circle and the scan direction indicated by an arrow).

of dot are presented in Fig. 2. The  $US_R$  was selected as the initial state [Fig. 2(a)]. At the first step, when the probe approaches the dot, part of magnetization vectors near the probe changes their orientation according to the probe magnetic field [Fig. 2(b)]. In the next stage vorticity state in the right part of dot starts to form [Fig. 2(c)]. As the probe moves to the central part vortexlike state is formed [Fig. 2(d)], which breaks up with spin flip in the bottom part of dot [Fig. 2(e)]. So we have  $US_L$  with opposite direction of magnetization. This algorithm was used for manipulation of magnetic moment in separate selected dots. Tapping/lift mode or constant height mode (with low scan height) scanning within one dot area was performed for switching of magnetization. The results of successive remagnetization of three dots are shown in Fig. 3. First, one dot was switched [shown by arrow in Fig. 3(a)], then second [Fig. 3(b)] and third one subsequently [Fig. 3(c)]. After that, the second dot was switched to the initial state [Fig. 3(d)].

So, the process can be used to control local magnetic field configuration in the arrays of magnetic nanodots. For

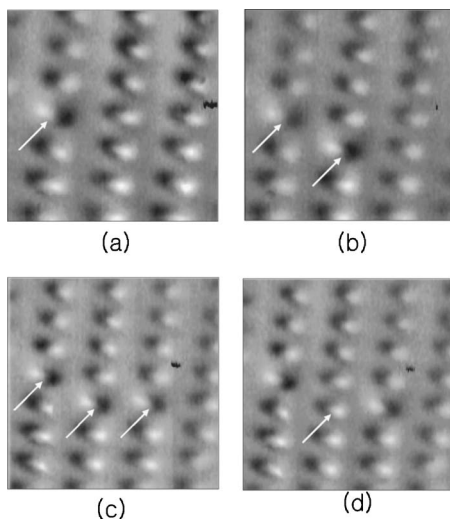


FIG. 3. Subsequent control of tip induced magnetization reversal process in FeCr nanodots. Scan area is  $4.5 \times 4.5 \mu\text{m}^2$ .

the purpose, one-dimensional arrays (chains) of elliptical Co dots with long axis perpendicular to the chain direction were formed near the Josephson junction.<sup>30</sup> The characteristic lateral sizes of dots were varied in the range of 100–600 nm, separation between particles was 100–500 nm. As was observed, the distribution of magnetic moments of particles in these one-dimensional chains strongly depends on the inter-dot distance. For the chains with separation less than 100 nm, we observed antiferromagnetic ordering of moments of dots in the remanent state. It is a result of magnetostatic interaction between dots. This interaction leads to unusual behavior of the system. Here, we concentrated our efforts on the experiments with dots, which had lateral sizes of  $300 \times 150 \text{ nm}^2$ , height of 10 nm, and separation of 150 nm. After magnetizing in the external field of 10 kOe in direction to long axis, this chain had a ferromagnetic order, as shown in MFM image [Fig. 4(a)]. In this state chain of particles has averaged magnetic field.

The probe induced antiferromagnetic ordering of this chain was performed in constant height mode. The height of scanning was reduced over selected dots until they change direction of magnetic moment to opposite. The distribution of local magnetic moments in dots after probe induced antiferromagnetic ordering can be seen in Fig. 4(b). In this state averaged magnetic field of dot row is equal to zero. Field

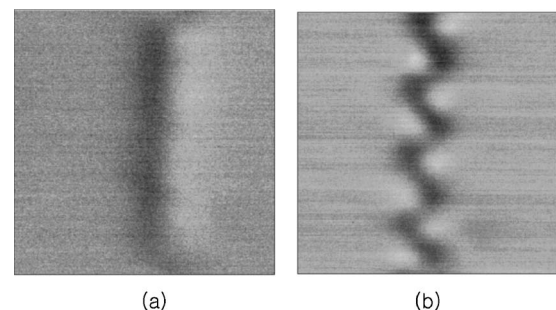


FIG. 4. MFM images of chain of Co dots after magnetizing in the external field of 10 kG (a) and after probe induced antiferromagnetic ordering (b). Scan area is  $3.5 \times 3.5 \mu\text{m}^2$ .

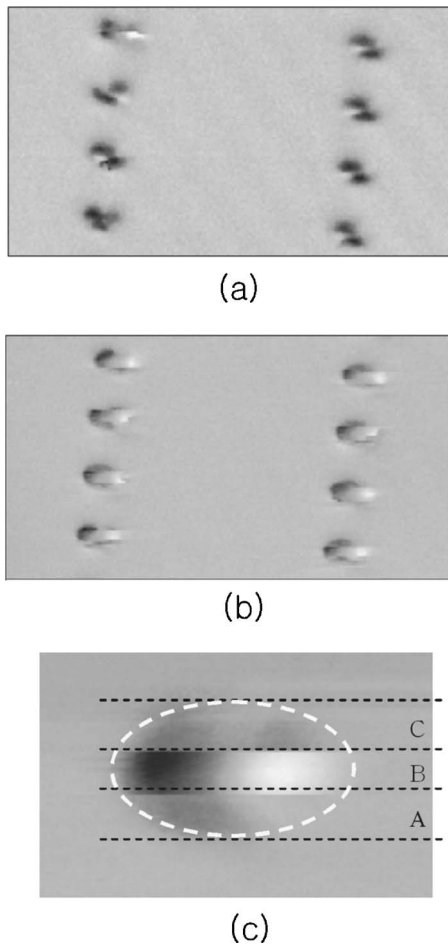


FIG. 5. Constant height mode MFM image of as-fabricated Co dots (a) and tapping/lift mode MFM image (b) of the Co dot array after transition to US. Scan area is  $7 \times 4 \mu\text{m}^2$ . (c) Enlarged tapping/lift mode MFM image of one Co dot.

switch on and switch off effects were clearly seen in the dependences of critical supercurrent of coplanar Josephson junction with ferromagnetic dots on external magnetic field.<sup>11</sup> The same principals can be used to control magnetic field in spintronics devices by means of switching magnetic moment of dots grown over the spin current channels.

### B. MFM probe induced $\text{VS}_R \Rightarrow \text{US} \Rightarrow \text{VS}_L$ transitions

As is well known, both US and VS can be realized in ferromagnetic small dots depending on the ratio of lateral size and height.<sup>31</sup> In the part, we used arrays of elliptical Co dots with lateral sizes of  $400 \times 600 \text{ nm}^2$ . Micromagnetic modeling<sup>32</sup> and MFM investigations show that for the dots there is a characteristic height  $h^*$  about 25 nm, which separates the regions of US and VS stabilities. When the height of dot  $h > h^*$ , US is getting unstable while VS becomes stable in the dots. For remagnetization experiments, 27 nm height slightly larger than  $h^*$  dot array were fabricated and the corresponding MFM images of Co dots are shown in Fig. 5. MFM image obtained by constant height mode indicates that the remanent magnetic state of the as-fabricated dots is VS. The symmetry of the MFM images for elliptical vortex corresponds to quadrupole and unambiguously defines the vorticity direction. In the tapping/lift mode for probes with a

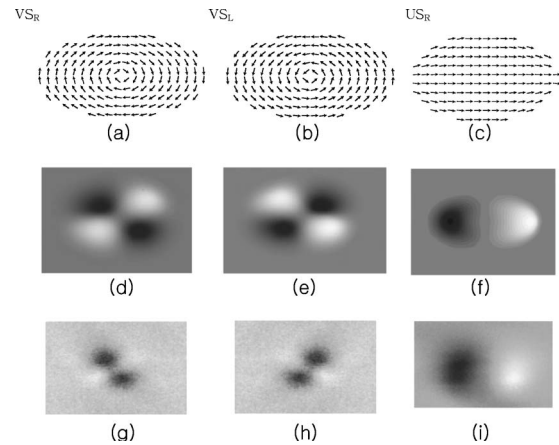


FIG. 6. The magnetization distribution [(a)–(c)], corresponding to MFM contrast calculated for  $\text{VS}_R$ ,  $\text{VS}_L$ , and US [(d)–(f)], and experimentally observed MFM contrast [(g)–(i)] of each corresponding magnetic state.

high magnetic moment we observed transitions between VS and US, which were registered as a sharp increase in the MFM contrast [Fig. 5(b)].

When the probe moved over the edge of a particle [region A in Fig. 5(c)], weak MFM contrast corresponding to VS was observed (scanning along the long axis of the dot). After that, during scanning in the central part of the dot (region B), the transition  $\text{VS} \Rightarrow \text{US}$  accompanied by an abrupt increase in the MFM signal was found. Eventually, when the probe passed over other edge (region C), a reversal transition  $\text{US} \Rightarrow \text{VS}$  was observed. It is noted that the uncontrolled  $\text{US} \Rightarrow \text{VS}$  switching was reported by some previous reports<sup>22,23,33</sup> as unsuccessful attempts to change the magnetization direction of US in high aspect ratio nanodots. However, the results presented in Figs. 5(b) and 5(c) suggest a different view of this situation. As clearly seen from the images, in the case of low aspect ratio dots the US is a metastable state and transitions  $\text{VS} \Rightarrow \text{US} \Rightarrow \text{VS}$  can be used to change the direction of a magnetic vortex.

Indeed symmetry of MFM images for elliptical vortices is clearly defined by vortex chirality. The magnetization distribution [(a)–(c)], corresponding to MFM contrast calculated for  $\text{VS}_R$ ,  $\text{VS}_L$ , and US [(d)–(f)], and experimentally observed MFM contrast [(g)–(i)] of each magnetic state are presented in Fig. 6. The typical black-white pole symmetry of the MFM images for elliptical vortex corresponds to quadrupole magnetic moment of magnetization distribution.<sup>4,5</sup>

We performed computer micromagnetic simulations of the remagnetization processes, which were observed in elliptical Co nanodots under magnetic field of the MFM probe. The vortex state  $\text{VS}_L$  was the initial state in calculations. When the probe moves along the central part of a dot, the vortex shifts to the edge [Figs. 7(a) and 7(b)] and is annihilated,<sup>34</sup> so that a uniform magnetization distribution appears in the area behind the probe [Figs. 7(c) and 7(d)]. The US is metastable in these dots. If the symmetry of US distribution is broken by scanning near the particle edge, a transition in the stable VS is observed. Formation of VS is defined by symmetry of the probe magnetic field and probe location near the dot. The  $\text{US} \Rightarrow \text{VS}$  process is illustrated in Fig. 8.

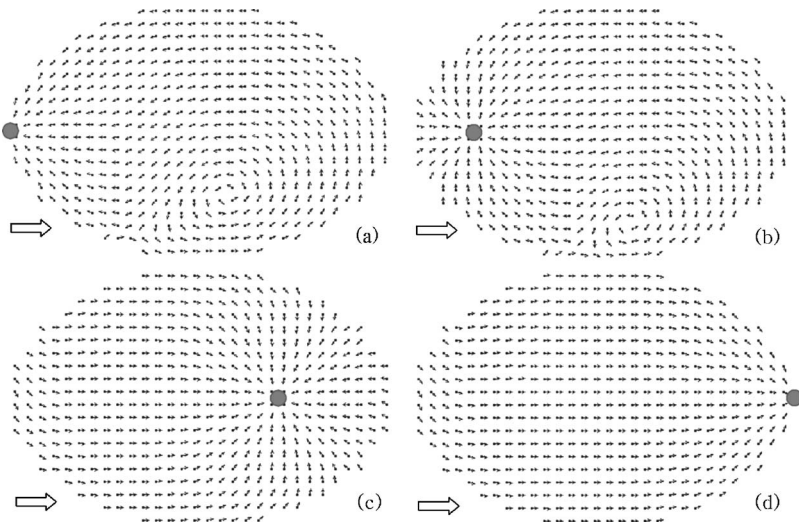


FIG. 7. The VS $\Rightarrow$ US transition under scanning of MFM probe (a gray circle indicates the probe position and the scan direction indicated by an arrow).

At the first stage, when the probe approaches the dot [Fig. 8(a)], vorticity of magnetization distribution with direction defined by the MFM probe field appears. This situation can be analyzed on the base of LLG equations. Actually, we can find solution in the form

$$\mathbf{M} = \mathbf{M}_U + \boldsymbol{\varepsilon},$$

where  $\mathbf{M}_U = (M_s, 0, 0)$  is the uniform magnetization and  $\boldsymbol{\varepsilon}$  is the infinitesimal perturbation. Omitting first term in LLG equation describing precession of magnetic moment, in first order of perturbation, we have the following equation for  $\text{rot } \boldsymbol{\varepsilon}$ :

$$\frac{d}{dt}(\text{rot } \boldsymbol{\varepsilon}) \cong - \frac{\alpha\gamma}{(1 + \alpha^2)M_s} [\nabla(\mathbf{M}_U \mathbf{H}) \times \mathbf{M}_U]. \quad (3)$$

After simple algebra, Eq. (3) takes the form

$$\left\langle \frac{d}{dt}(\text{rot } \boldsymbol{\varepsilon})_z \right\rangle \cong \frac{\alpha\gamma}{(1 + \alpha^2)M_s} \left\langle \frac{\partial H_x}{\partial y} \right\rangle,$$

where volume averaging is indicated as  $\langle \rangle$ . As clearly seen, the averaged Z component of vorticity for the initial stage is determined by inhomogeneity of the x component of the

MFM probe field. We can see also that the direction of the vorticity depends on the sign of the asymmetry of distribution of external magnetic field. From this point of view, the situation presented in Fig. 8(a) corresponds to the vortex nucleation with the clockwise orientation. On the other hand, it is clear that question about vortex formation is nonlinear problem, which can be considered correctly only by computer simulation.

As the probe passed over the dot a characteristic fold of magnetization is formed near the dot boundary [marked by a black arrow in Fig. 8(b)]. The VS is nucleated in this fold, as shown in Fig. 8(c). After nucleation, the vortex shifts quickly to the center of dot while the probe goes out. The modeling results show that the vorticity direction in the US $\Rightarrow$ VS process is determined by the position of probe relative to dot. According to the situation presented in Fig. 8, if the probe moves along the bottom region of dot, a vortex nucleates with the clockwise orientation. In the opposite case, when the probe is moved along the top edge of particle, the micro-magnetic simulation shows that the vortex nucleation with the counterclockwise orientation is observed. Such processes can be used to control the vorticity direction of a magnetic

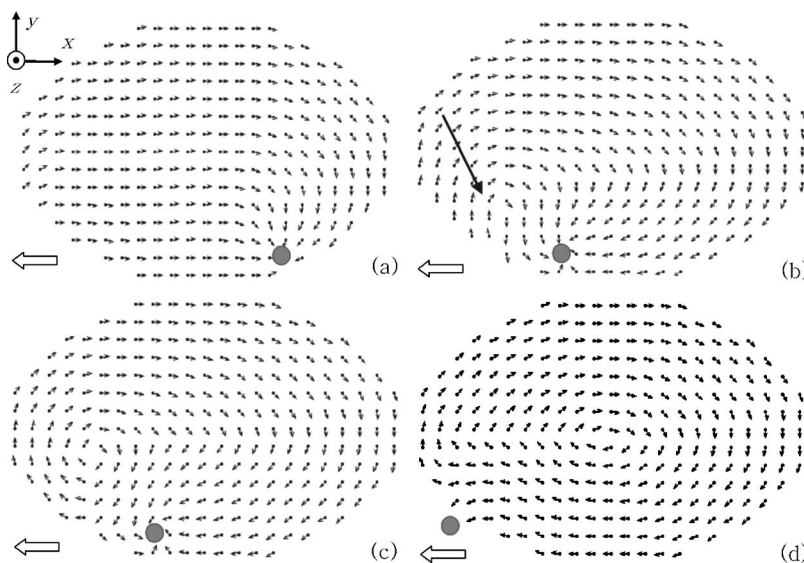


FIG. 8. The transition of US $\Rightarrow$ VS under scanning of MFM probe (the scan direction indicated by a thick arrow).

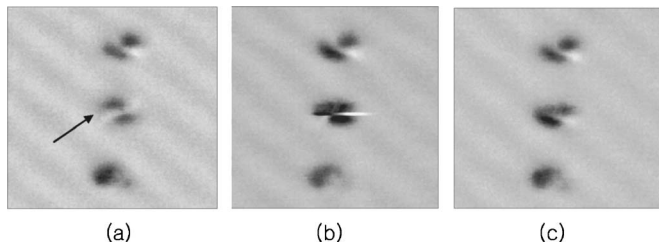


FIG. 9. Switching of vorticity direction within a Co dot (central dot). (a) Constant height MFM image of the initial state. (b) MFM image obtained by scanning with variable height. (c) The final state. Scan area is  $3 \times 3 \mu\text{m}^2$ .

vortex. Indeed, our experiments show that vorticity orientation can be changed during scanning over a dot by a special algorithm. MFM images of the three dot region that illustrate the vortex direction switching by the  $\text{VS} \Rightarrow \text{US} \Rightarrow \text{US} \Rightarrow \text{VS}$  transitions are presented in Fig. 9.

The initial state of the central dot in Fig. 9(a) marked as an arrow corresponds to the clockwise orientation of vortex. The next image [Fig. 9(b)] was obtained in the following way. At the first stage, scanning was performed in the constant height mode with a probe-surface distance of about 50 nm. When the probe passed over the central dot, the scanning height was reduced to 15 nm and  $\text{VS} \Rightarrow \text{US}$  transition was found. Afterwards, when the probe reached the edge,  $\text{US} \Rightarrow \text{VS}$  transition was observed whereupon the probe was lifted to 50 nm height again. The final state with the counterclockwise vortex orientation in central dot is presented in Fig. 9(c).

The MFM probe induced  $\text{US} \Rightarrow \text{VS}$  transitions were used to control local magnetic field configuration in the arrays of magnetic nanodots. In particular, such methods were applied to change the field distribution in the plane overlapping Josephson junctions.<sup>13</sup> For these purposes two-dimensional arrays of elliptical Co dots were formed just over the Josephson junction. The characteristic lateral sizes of dots were  $300 \times 600 \text{ nm}^2$ , height of 25 nm. After magnetizing in the external field of 10 kOe in direction to the long axis, all dots had the uniform magnetization as it is shown in MFM image [Fig. 10(a)]. In this state array of dots induced sufficiently strong magnetic field.

The probe induced  $\text{US} \Rightarrow \text{VS}$  demagnetization (transition to the vortex state with low magnetic field) in the selected sample area was performed in the tapping/lift mode. The distribution of local magnetic moments in dots after probe

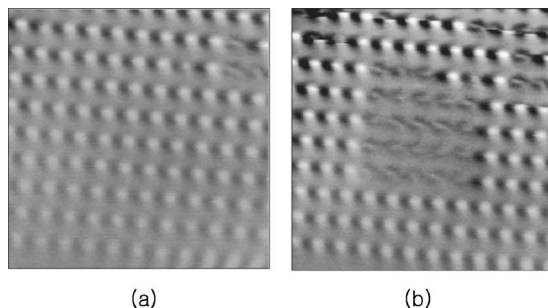


FIG. 10. MFM images of Co dot array after magnetizing in the external 10 kOe field (a) and after MFM probe induced  $\text{US} \Rightarrow \text{VS}$  demagnetization (b). Scan area is  $15 \times 15 \mu\text{m}^2$ .

induced  $\text{US} \Rightarrow \text{VS}$  demagnetization shown in MFM image [Fig. 10(b)]. In this state magnetic field induced by the dots is very small. Field switch on and switch off effects were clearly observed in overlapping Josephson junctions as the giant variations of the maximum critical current in the dependences of critical current on external magnetic field.<sup>13</sup>

## V. CONCLUSION

In conclusion, we demonstrate the possibility to control the magnetic state of ferromagnetic nanodots by inhomogeneous magnetic field produced by probe of magnetic force microscope. The geometrical size and shape of dot in combination with various methods of MFM probe manipulation allow to realize different  $\text{US}_R \Leftrightarrow \text{US}_L$ ,  $\text{US} \Leftrightarrow \text{VS}$ , and  $\text{VS}_R \Rightarrow \text{US} \Rightarrow \text{VS}_L$  transitions in magnetization distribution of the dots. Using computer calculations, we have demonstrated that process of magnetization reversal of ferromagnetic nanodots under the action of magnetic probe has a complicated character and scenario of the process is different in principle from the behavior of the system in homogeneous magnetic field. On the other hand, we formulated simple rules for manipulation of magnetic state of ferromagnetic nanodots using probe of MFM and demonstrated possibilities for the creation of different distributions of magnetic field induced by arrays of ferromagnetic nanodots. This is a very effective way to control switching properties of different objects. First of all, it is applicable to objects with strong magnetic susceptibility such as superconductors and semiconductors with giant Zeeman splitting.

## ACKNOWLEDGMENTS

This work was partly supported by Korea-Russia International Cooperation Program in KIST (2Z02660), RFBR, INTAS (03-51-6426 and 03-51-4778), and ISTC (2976). The authors are very thankful to V. B. Shevtsov for help in MFM measurements, to N. I. Polushkin and Yu. K. Verevkin for assistance in sample fabrication, and to D. S. Nikitushkin, I. R. Karetnikova, I. M. Nefedov, and I. A. Shereshevsky for assistance in computer simulations.

- <sup>1</sup>J. I. Martin, J. Nogues, K. Liu, J. L. Vicent, and I. K. Schuller, *J. Magn. Magn. Mater.* **256**, 449 (2003).
- <sup>2</sup>A. M. Kosevich, M. P. Voronov, and I. V. Marjos, *JETP* **57**, 86 (1983).
- <sup>3</sup>R. P. Cowburn, D. K. Koltsov, A. O. Adeyeye, M. E. Welland, and D. M. Tricker, *Phys. Rev. Lett.* **83**, 1042 (1999).
- <sup>4</sup>A. Fernandez and C. J. Cerjan, *J. Appl. Phys.* **87**, 1395 (2000).
- <sup>5</sup>T. Okuno, K. Shigeto, T. Ono, K. Mibu, and T. Shinjo, *J. Magn. Magn. Mater.* **240**, 1 (2002).
- <sup>6</sup>A. A. Fraerman *et al.*, *Phys. Low-Dim. Struct.* **1/2**, 35 (2004).
- <sup>7</sup>Y. Otani, B. Pannetier, J. P. Nozieres, and D. Givord, *J. Magn. Magn. Mater.* **126**, 622 (1993).
- <sup>8</sup>O. Geoffroy, D. Givord, Y. Otani, B. Pannetier, and F. Ossart, *J. Magn. Magn. Mater.* **121**, 223 (1993).
- <sup>9</sup>J. I. Martin, M. Velez, J. Nogues, and I. K. Schuller, *Phys. Rev. Lett.* **79**, 1929 (1997).
- <sup>10</sup>A. V. Silhanek, L. Van Look, S. Raedts, R. Jonckheere, and V. V. Moshchalkov, *Phys. Rev. B* **68**, 214504 (2003).
- <sup>11</sup>A. Y. Aladyshkin, A. A. Fraerman, S. A. Gusev, A. Y. Klimov, Y. N. Nozdrin, G. L. Pakhomov, V. V. Rogov, and S. N. Vdovichev, *J. Magn. Magn. Mater.* **258–259**, 406 (2003).
- <sup>12</sup>S. N. Vdovichev, S. A. Gusev, Yu. N. Nozdrin, A. V. Samokhvalov, A. A. Fraerman, E. Il'ichev, R. Stolz, and L. Fritzsche, *J. Magn. Magn. Mater.* **300**, 202 (2006).

- <sup>13</sup>S. N. Vdovichev *et al.*, JETP Lett. **80**, 651 (2004).
- <sup>14</sup>M. Berciu and B. Janko, Phys. Rev. Lett. **90**, 246804 (2003).
- <sup>15</sup>T. Dietl, M. Sawicki, M. Dahl, D. Heiman, E. D. Isaacs, M. J. Graf, S. I. Gubarev, and D. L. Alov, Phys. Rev. B **43**, 3154 (1991).
- <sup>16</sup>R. Merservey, D. Paraskevopoulos, and P. M. Tedrow, Phys. Rev. B **22**, 1331 (1980).
- <sup>17</sup>V. A. Vas'ko, V. A. Larkin, P. A. Kraus, K. R. Nikolaev, D. E. Grupp, C. A. Nordman, and A. M. Goldman, Phys. Rev. Lett. **78**, 1134 (1997).
- <sup>18</sup>F. J. Jedema, M. S. Nijboer, A. T. Filip, and B. J. van Wees, Phys. Rev. B **67**, 085319 (2003).
- <sup>19</sup>V. V. Ryazanov, V. A. Oboznov, A. S. Prokofiev, and S. V. Dubonos, JETP Lett. **77**, 39 (2003).
- <sup>20</sup>I. Zutic, J. Fabian, and S. Das Sarma, Rev. Mod. Phys. **76**, 323 (2004).
- <sup>21</sup>M. Kleiber, F. Kümmerlen, M. Löhndorf, A. Wadas, D. Weiss, and R. Wiesendanger, Phys. Rev. B **58**, 5563 (2002).
- <sup>22</sup>X. Zhu, P. Grütter, V. Metlushko, and B. Ilic, Phys. Rev. B **66**, 024423 (2002).
- <sup>23</sup>X. Zhu, P. Grütter, V. Metlushko, and B. Ilic, J. Appl. Phys. **91**, 7340 (2002).
- <sup>24</sup>M. Shneider, H. Hofman, and J. Zweck, Appl. Phys. Lett. **79**, 3113 (2001).
- <sup>25</sup>A. A. Fraerman *et al.*, Phys. Rev. B **65**, 064424 (2002).
- <sup>26</sup>A. M. Alexeev, Yu. V. Verevkin, N. V. Vostokov, V. N. Petrjakov, N. I. Polushkin, A. F. Popkov, and N. N. Salashchenko, JETP Lett. **73**, 214 (2001).
- <sup>27</sup>E. D. Boerner and H. N. Bertran, IEEE Trans. Magn. **33**, 3152 (1997).
- <sup>28</sup>U. Hartmann, Phys. Lett. A **137**, 475 (1989).
- <sup>29</sup>Th. Kebe and A. Carla, J. Appl. Phys. **95**, 775 (2004).
- <sup>30</sup>A. A. Fraerman and M. V. Sapozhnikov, Phys. Rev. B **65**, 184433 (2002).
- <sup>31</sup>I. L. Prejbeanu, N. Natali, L. D. Buda, U. Ebels, A. Lebib, Y. Chen, and K. Ounadjela, J. Appl. Phys. **91**, 7343 (2002).
- <sup>32</sup><http://math.nist.gov/oommf>
- <sup>33</sup>A. Fernandez, M. R. Gibbons, M. R. Wall, and C. J. Cerjan, J. Magn. Magn. Mater. **190**, 71 (1998).
- <sup>34</sup>K. Yu. Guslienko, V. Novosad, Y. Otani, H. Shima, and K. Fukamichi, Phys. Rev. B **65**, 024414 (2001).